Macromolecules

COMMUNICATION TO THE EDITOR

pubs.acs.org/Macromolecules

On Micellar Exchange: The Role of the Insertion Penalty

A. Halperin*

Univ. Grenoble 1/CNRS, LIPhy UMR 5588, Grenoble, F-38041, France

The near-equilibrium relaxation kinetics of diblock copolymer micelles is among the simplest of the different scenarios encountered in the dynamics of copolymeric mesophases.[1,2] Even in this limit, there is no full consensus on the underlying physics. Experimentally, the kinetics can be studied using time-resolved small-angle neutron scattering (TR-SANS), probing the redistribution of deuterated and nondeuterated chains among micelles dispersed in a selective solvent.[3−8] The various experiments suggest that the relaxation proceeds by exchange of single diblock copolymer chains, unimers, as was suggested by theory.[9] The exchange is activation process, and the results were interpreted assuming an expulsion rate constant of the form $k_{ex} \sim \exp(-F_a/kT)$. The activation free energy associated with the expulsion of the insoluble B block out of the micellar core, F_a, was represented by a single term scaling with the polymerization degree of the B block, N_B, as $F_a \sim N_B{}^x$. However x and the numerical prefactor are subject of debate. Two forms of F_a allow to fit the experimental data: (i) One, with $x = 2/3$,[7] corresponds to the surface free energy of a collapsed B block in the solvent swollen corona[9−11] $\gamma_B N_B{}^{2/3} a^2$ where γ_B is the surface tension of the collapsed B block and a is the monomer size. (ii) The second, with $x = 1$, assumes that the expelled B block remains swollen and attributes F_a to monomer−solvent contacts via $kT\chi N_B$ where χ is the Flory−Huggins interaction parameter.[8] This controversy is further complicated by the recent observation by Choi et al.[12] of a significant slowdown of the relaxation rate in micellar solutions of higher concentration where coronal overlap results in micellar ordering and growth. The slowdown is difficult to rationalize in terms of the two F_a noted earlier.

This Communication aims to suggest a possible mechanism of the slowdown arguing that F_a reflects two contributions, $F_a = F_0 + \Delta F$: The first and leading term, $F_0 \approx \gamma_B N_B{}^{2/3} a^2$, allows for the surface energy of the expelled B block, "bud", forming a spherical globule of radius $r_{bud} \approx N_B{}^{1/3} a$. This familiar term is independent of the equilibrium aggregation number f_{eq} and the micellar morphology. The second term, ΔF, reflects two corrections: (i) the osmotic penalty incurred upon inserting the impenetrable bud within the interior of the corona and (ii) the change in the micellar free energy due to the creation of the bud. ΔF, in contrast to F_0, increases with f_{eq}, thus providing a possible rationalization for the slowdown of the exchange kinetics.

For brevity, I limit the discussion to F_a of starlike micelles[13,14] in a highly selective solvent that is athermal for the coronal A block and nonsolvent for the core B block. In this limit the polymerization degree of the coronal A blocks, N_A, is much higher than that of the B blocks, $N_B \ll N_A$, and the corona is described by the Daoud−Cotton star model;[15,16] i.e., it comprises spherical shells of closed packed blobs of size $\xi \approx r/f^{1/2}$ with a free energy per coronal A block $F_{corona}/kT \approx f^{1/2} x_0$ with $x_0 = \ln(R_{corona}/R_{core})$. At equilibrium F_{corona} is comparable to the surface free energy per core B block, $F_{surf}/kT \approx \gamma N_B{}^{2/3}/f^{1/3}$ where $\gamma \equiv \gamma_B a^2/kT$. Accordingly, $f_{eq} \approx (\gamma/x_0)^{6/5} N_B{}^{4/5}$, leading to a core radius $R_{core} \approx (\gamma/x_0)^{2/5} N_B{}^{3/5}$ and a micellar radius $R_{mic} \approx f_{eq}{}^{1/5} N_A{}^{3/5} \approx (\gamma/x_0)^{6/25} N_B{}^{4/25} N_A{}^{3/5}$. The spans of the innermost and outermost blobs are respectively $\xi_{in}/a \approx (\gamma/x_0)^{-1/5} N_B{}^{1/5}$ and $\xi_{out}/a \approx (\gamma/x_0)^{-9/25} N_B{}^{-6/25} N_A{}^{3/5}$, thus defining the corresponding A monomer volume fractions $\varphi* = \varphi_A(R_{micelle}) \approx (\gamma/x_0)^{12/25} N_B{}^{8/25} N_A{}^{-4/5}$ and $\varphi** = \varphi_A(R_{core}) \approx (\gamma/x_0)^{4/15} N_B{}^{-4/15}$. The starlike limit is attained in the systems studied by Lund et al.[3,5−7] where $N_A/N_B \simeq 25$, while the micelles investigated by Choi et al.[8,12] with $2 \lesssim N_A/N_B \lesssim 4$ are less asymmetric.

Consider now the activated state for the expulsion of a unimer from a starlike micelle with $f = f_{eq} \gg 1$. It is assumed to consist of a core comprising $f_{eq} - 1$ B blocks with a collapsed bud at grazing contact with the core[9] (Figure 1). The corona is essentially unperturbed apart from displacement of the A block of the expelled unimer by r_{bud}. The following terms contribute to ΔF: (i) The lowering of the surface free energy of the core due to the decrease of its surface area $\Delta F_{surf} = F_{surf}(f_{eq} - 1) - F_{surf}(f_{eq}) \approx \gamma N_B{}^{2/3} f_{eq}{}^{2/3}[(1 - f_{eq}{}^{-1})^{2/3} - 1] \approx - \gamma N_B{}^{2/3}/f_{eq}{}^{1/3} \approx -\gamma^{3/5} N_B{}^{2/5}$. (ii) The increase in the total free energy of the corona, $f^{3/2} \ln(R_{micelle}/R_{core})$ dues to the lowering of the core radius from R_{core} to $\overline{R}_{core} \approx (f_{eq} - 1)^{1/3} N_B{}^{1/3}$ leading to $\Delta F_{corona} = F_{corona}(\overline{R}_{core}) - F_{corona}(R_{core}) \approx f_{eq}{}^{3/2} \ln(R_{core}/\overline{R}_{core}) \approx f_{eq}{}^{1/2} \approx \gamma^{3/5} N_B{}^{2/5}$. (iii) The work of inserting an impenetrable particle against the osmotic pressure of the coronal ΔF_{ins}. The kT per blob prescription together with the Daoud−Cotton model specify the coronal osmotic pressure $\Pi(r) \approx kT/\xi(r)^3 \approx kTf_{eq}{}^{3/2}/r^3 \approx kTN_B{}^{6/5}/r^3$. Since $r_{bud} > \xi_{in}$, ΔF_{ins} for inserting the bud at $r = R_{core} + r_{bud} \ll R_{mic}$ is roughly

$$\Delta F_{ins}/kT \approx r_{bud}{}^2 \int_{\overline{R}_{core}}^{\overline{R}_{core} + 2r_{bud}} \Pi(r)\, dr$$

$$\approx f_{eq}{}^{3/2} \frac{r_{bud}^2}{2\overline{R}_{core}^2} \left[1 - \left(\frac{\overline{R}_{core}}{\overline{R}_{core} + 2r_{bud}} \right)^2 \right] \qquad (1)$$

In the $r_{bud} \ll R_{core}$ limit the leading term is $\Delta F_{ins}/kT \approx f_{eq}{}^{3/2}(r_{bud}/\overline{R}_{core})^3 \approx f_{eq}{}^{3/2}(r_{bud}/R_{core})^3(1 + f_{eq}{}^{-1})$ or $\Delta F_{ins}/kT \approx (r_{bud}/\xi_{in})^3$. Accordingly, for dilute solutions of nonoverlapping starlike micelles, when $\xi_{in}/a \approx \gamma^{-1/5} N_B{}^{1/5}$, eq 1 leads to $\Delta F_{ins}/kT \approx \gamma^{3/5} N_B{}^{2/5}$. While ΔF_{ins} was invoked in discussions of

Received: April 8, 2011
Revised: June 1, 2011
Published: June 10, 2011

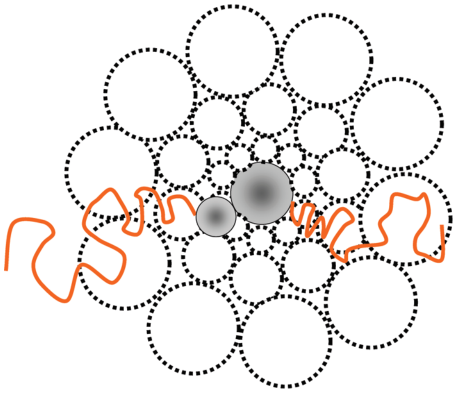

Figure 1. Schematic view of an activated state for the expulsion of a unimer out of a starlike micelle comprising f_{eq} AB diblocks in a dilute micellar solution. It comprises a core of $f_{\mathrm{eq}} - 1$ B blocks with a collapsed B block, "bud", at grazing contact with the core. The starlike coronal structure is weakly modified because of the smaller core radius. The bud is larger than the innermost blob. Representative coronal A blocks are depicted in red, and the blobs are depicted as circles with dashed boundaries.

protein–brush interactions[17] and is supported by computer simulations,[18–20] it was not considered thus far in the context of micellar exchange. Altogether $\Delta F \approx \gamma^{3/5} N_{\mathrm{B}}^{2/5}$ and $F_{\mathrm{a}} = F_0 + \Delta F$ is

$$\begin{aligned} F_{\mathrm{a}}/kT &\approx \gamma N_{\mathrm{B}}^{2/3} + \gamma^{3/5} N_{\mathrm{B}}^{2/5} \\ &= \gamma N_{\mathrm{B}}^{2/3}[1 + \gamma^{-2/5} N_{\mathrm{B}}^{-4/15}] \end{aligned} \tag{2}$$

The F_0 term thus dominates the scaling behavior of F_{a} while the ΔF term can manifest itself as a correction to the numerical prefactor preceding $\gamma N_{\mathrm{B}}^{2/3}$. For example, in the interval $N_{\mathrm{B}} = 200-400$ explored by Choi et al.[12] $N_{\mathrm{B}}^{-4/15}$ varies in the range 0.2–0.24. It is however important to note that fitting the measured relaxation rate $R(t)$ data is highly sensitive to the value of numerical factors since it involves a double exponential

$$R(t) = \int_1^{\infty} P(N_{\mathrm{B}}) \exp(-k_{\mathrm{ex}} t)\, \mathrm{d}N_{\mathrm{B}} \tag{3}$$

where $P(N_{\mathrm{B}})$ characterizes the polydispersity of the core blocks.[5,7,8] In addition, note the difference with respect to the insertion a sphere of radius R into a bulk semidilute solution where $\Delta F_{\mathrm{surf}}/\Delta F_{\mathrm{ins}} \approx \gamma R^2/\Pi R^3 \sim 1/R$ and ΔF_{ins} dominates at high R. In our discussion the opposite trend occurs because both R and Π vary with N_{B}.

The ΔF_{ins} term leads to qualitatively novel features when the micellar concentration exceeds the overlap threshold and the A monomer volume fraction, φ_{A}, exceeds $\varphi*$. We first summarize the φ_{A} effects on the micellar structure[14] noting that they may also result from adding A homopolymer.[24] In the $\varphi* < \varphi < \varphi**$ range the corona develops two regions:[14,15] (i) an exterior "bulklike" region of blobs of constant size $\xi_{\mathrm{A}} \approx \varphi_{\mathrm{A}}^{-3/4} a$ comprising each of $g_{\mathrm{A}} \approx \varphi_{\mathrm{A}}^{-5/4}$ monomers, occurring because coronal overlap introduces additional screening of excluded volume interactions. (ii) An interior region with a star like structure and $\xi \approx r/f_{\mathrm{eq}}^{1/2}$. The boundary between the two regions occurs at $r_{\mathrm{co}} \approx f_{\mathrm{eq}}^{1/2} \xi_{\mathrm{A}} \approx N_{\mathrm{B}}^{2/5} \varphi_{\mathrm{A}}^{-3/4} a$. At $\varphi_{\mathrm{A}} \approx \varphi**$, when $r_{\mathrm{co}} \approx R_{\mathrm{core}}$, the whole coronal star structure disappears. In the $\varphi* < \varphi < \varphi**$ range the free energy per A block assumes the form[14]

$$F_{\mathrm{corona}}/kT \approx f^{1/2} \ln \frac{r_{\mathrm{co}}}{R_{\mathrm{core}}} + f^{1/2}\left(1 - \frac{r_{\mathrm{co}}}{R_{\mathrm{micelle}}}\right) + \frac{N_{\mathrm{A}} - N_{\mathrm{int}}}{g_{\mathrm{A}}} \tag{4}$$

The first term accounts for the free energy per chain within the inner starlike region, comprising $N_{\mathrm{int}} < N_{\mathrm{A}}$ monomers,[21] by assigning kT per blob. The second term reflects the extension free energy of a chain segment in the exterior region viewed as a Gaussian string of $(N_{\mathrm{A}} - N_{\mathrm{int}})/g_{\mathrm{A}}$ blobs of size ξ_{A}.[22] The third term accounts for the interaction free energy, kT per blob, of the exterior segment. For $R_{\mathrm{core}} \ll r_{\mathrm{co}} \ll R_{\mathrm{micelle}}$ the first and third terms dominate. However, the third term is only weakly dependent on the structure of the micelles since the major contribution is due to $N_{\mathrm{A}} \varphi_{\mathrm{A}}^{5/4}$ because a single "star" blob is replaced by a number of ξ_{A} blobs. Overall, the structure of the micelle is thus determined by the balance of $F_{\mathrm{surf}}/kT \approx \gamma N_{\mathrm{B}}^{2/3}/f^{1/3}$ and $F_{\mathrm{corona}}/kT \approx f^{1/2} \ln(r_{\mathrm{co}}/R_{\mathrm{core}}) \equiv f^{1/2} x$ where $x = \ln(\varphi**/\varphi_{\mathrm{A}})$. In other words, the scaling behavior of the micelles is modified because x_0 is replaced by the smaller and φ_{A} dependent $x(\varphi_{\mathrm{A}})$, thus leading to higher $f_{\mathrm{eq}} \approx (\gamma/x)^{6/5} N_{\mathrm{B}}^{4/5}$ and $R_{\mathrm{core}} \approx (\gamma/x)^{2/5} N_{\mathrm{B}}^{3/5}$.[14] Further increase in φ_{A}, when $\varphi_{\mathrm{A}} > \varphi**$, will affect the scaling behavior since the coronal penalty term will be eventually overtaken by the stretching elasticity of the core blocks $kTR_{\mathrm{core}}^2/N_{\mathrm{B}} a^2$, thus leading to crew cut scaling $f_{\mathrm{eq}} \approx \gamma N_{\mathrm{B}}$ and $R_{\mathrm{core}} \approx \gamma^{1/3} N_{\mathrm{B}}^{2/3} a$.[14] However, the $\varphi_{\mathrm{A}} > \varphi**$ range may involve morphological changes beyond the scope of this discussion.[23]

Increasing φ_{A} beyond $\varphi*$ weakly affects the F_0 term in F_{a} via the φ_{A} dependence of γ. It has however a significant effect on $\Delta F/kT \approx f_{\mathrm{eq}}^{1/2}$. In the $\varphi* < \varphi_{\mathrm{A}} \ll \varphi**$ range it increases because of the screening induced micellar growth. Since we have in mind TR-SANS experiments it is convenient to express this effect in terms of R_{core} because $R(t)$ and R_{core} can be measured independently. In particular, $f_{\mathrm{eq}} \approx R_{\mathrm{core}}^3/N_{\mathrm{B}} a^3$ leads to $\Delta F/kT \approx R_{\mathrm{core}}^{3/2}/N_{\mathrm{B}}^{1/2} a^{3/2}$ and eq 2 assumes the form

$$F_{\mathrm{a}}/kT \approx \gamma N_{\mathrm{B}}^{2/3} + R_{\mathrm{core}}^{3/2}(\varphi_{\mathrm{A}})/N_{\mathrm{B}}^{1/2} a^{3/2} \tag{5}$$

highlighting the φ_{A} dependence of ΔF. In this form eq 5 applies to micelles experiencing screening due to either added homopolymer or to overlap between micellar coronas. The effect on the kinetics is apparent from the ratio between the screened and unscreened rate constants, $k_{\mathrm{ex}}(\varphi_{\mathrm{A}})$ and $k_{\mathrm{ex}}(\varphi_{\mathrm{A}} = 0)$. In particular, $k_{\mathrm{ex}}(\varphi_{\mathrm{A}})/k_{\mathrm{ex}}(\varphi_{\mathrm{A}} = 0) \approx \exp\{-[F_{\mathrm{a}}(\varphi_{\mathrm{A}}) - F_{\mathrm{a}}(\varphi_{\mathrm{A}} = 0)]\}/kT \approx \exp\{-[\Delta F(\varphi_{\mathrm{A}}) - \Delta F(\varphi_{\mathrm{A}} = 0)]\}/kT$ or

$$\frac{k_{\mathrm{ex}}(\varphi_{\mathrm{A}})}{k_{\mathrm{ex}}(\varphi_{\mathrm{A}} = 0)} \approx \exp\left[-\frac{R_{\mathrm{core}}^{3/2}(\varphi_{\mathrm{A}} = 0)}{N_{\mathrm{B}}^{1/2} a^{3/2}} \left(\frac{R_{\mathrm{core}}^{3/2}(\varphi_{\mathrm{A}})}{R_{\mathrm{core}}^{3/2}(\varphi_{\mathrm{A}} = 0)} - 1\right)\right] \tag{6}$$

The k_{ex} values are very sensitive to γ that strongly affects both F_0 and ΔF. This is also manifested in $k_{\mathrm{ex}}(\varphi_{\mathrm{A}})/k_{\mathrm{ex}}(\varphi_{\mathrm{A}} = 0)$. The experimental observations indicate that the screened R_{core} is 20–30% larger, thus suggesting a rough estimate of $R_{\mathrm{core}}^{3/2}(\varphi_{\mathrm{A}})/R_{\mathrm{core}}^{3/2}(\varphi_{\mathrm{A}} = 0) - 1 \approx 1.25^{3/2} - 1 \approx 0.4$. The γ dependence of the $k_{\mathrm{ex}}(\varphi_{\mathrm{A}})/k_{\mathrm{ex}}(\varphi_{\mathrm{A}} = 0)$ is due to $R_{\mathrm{core}}^{3/2}(\varphi_{\mathrm{A}} = 0)/a^{3/2} N_{\mathrm{B}}^{1/2} \approx (\gamma/x_0)^{3/5} N_{\mathrm{B}}^{2/5}$. Thus, utilizing the upper limit of $\gamma/x_0 = 1$ for $N_{\mathrm{B}} = 400$ leads to $N_{\mathrm{B}}^{2/5} \approx 11$ and reduction of k_{ex} by a factor of $\exp(-4.4) \simeq 0.01$ strongly repressing the micellar exchange. However, $x_0 > 1$ and typically $\gamma < 1$ thus suggesting $\gamma/x_0 < 1$. For example, an estimate $\gamma/x_0 \simeq 0.3$[23] leads to lowering k_{ex} by a factor of $\exp(-2.2) \simeq 0.1$ comparable in order of magnitude to the experimental effect reported.[12] Detailed confrontation with experiment requires a more elaborate analysis allowing for the solvent content in the core, a better estimate of γ, and a quantitative expression for $\Pi(\varphi)$ appropriate to the experimental system.[23] Assuming no morphological changes occur, eqs 5 and 6 apply until $\varphi = \varphi**$ is reached, and ΔF for higher φ_A is determined the bulk osmotic pressure with $F_{ins} \approx r_{bud}{}^3\Pi(\varphi_A) \approx kTN_B\varphi_A{}^{9/4}$. If morphological changes do occur, eqs 5 and 6 apply to the $\varphi_A > \varphi**$ range corresponding to spherical micelles. The expulsion rate constant for different morphologies will have similar form, with an identical F_0 but with slightly modified ΔF.

Our discussion suggests the hypothesis that micellar exchange slows down because of coronal screening and the resulting increase in the osmotic pressure encountered by the expelled bud. For typical situations this increase is signaled by a concurrent increase in R_{core}. The screening can result from coronal overlap due to increase in the micelle concentration, as reported by Choi et al.[12] It can also result from addition A homopolymer to dilute solutions of nonoverlapping micelles. A homopolymer induced increase in R_{core}, predicted theoretically,[24] was observed experimentally.[25,26] It thus suggests experimental study of the effects of added homopolymer on the rate of unimer exchange between micelles. In such systems it is however necessary to allow for possible modifications of the micellar order because of depletion interactions.[25−27]

AUTHOR INFORMATION

Corresponding Author

*E-mail: avraham.halperin@ujf-grenoble.fr.

ACKNOWLEDGMENT

I acknowledge with thanks insightful discussions with E. B. Zhulina.

REFERENCES

(1) Denkova, A. G.; Mendes, E.; Coppens, M.-O. *Soft Matter* **2010**, *6*, 2351.

(2) Nicolai, T.; Colombani, O.; Chassenieux, C. *Soft Matter* **2010**, *6*, 3111.

(3) Willner, L.; Poppe, A.; Allgaier, J.; Monkenbusch, M.; Richter, D. *Europhys. Lett.* **2001**, *55*, 667.

(4) Won, Y. Y.; Davis, H. T.; Bates, F. S. *Macromolecules* **2003**, *36*, 953.

(5) Lund, R.; Willner, L.; Stellbrink, J.; Lindner, P.; Richter, D. *Phys. Rev. Lett.* **2006**, *96*, 068302.

(6) Lund, R.; Willner, L.; Richter, D.; Dormidontova, E. E. *Macromolecules* **2006**, *39*, 4566.

(7) Lund, R.; Willner, L.; Stellbrink, J.; Lindner, P.; Richter, D. *Phys. Rev. Lett.* **2010**, *104*, 049902.

(8) Choi, S.-H.; Lodge, T. P.; Bates, F. S. *Phys. Rev. Lett.* **2010**, *104*, 047802.

(9) Halperin, A.; Alexander, S. *Macromolecules* **1989**, *22*, 2403.

(10) Dormidontova, E. E. *Macromolecules* **1999**, *32*, 7630.

(11) Nose, T.; Iyama, K. *Comput. Theor. Polym. Sci.* **2000**, *10*, 249.

(12) Choi, S.-H.; Bates, F. S.; Lodge, T. P. *Macromolecules* **2011**, *44*, 3594.

(13) Halperin, A. *Macromolecules* **1987**, *20*, 2943.

(14) Birshtein, T. M.; Zhulina, E. B. *Polymer* **1989**, *30*, 170.

(15) Daoud, M.; Cotton, J. P. *J. Phys. (Paris)* **1982**, *43*, 531.

(16) Birshtein, T. M.; Zhulina, E. B. *Polymer* **1986**, *27*, 1078.

(17) Halperin, A.; Fragneto, G.; Schollier, A.; Sferrazza, M. *Langmuir* **2007**, *23*, 10603.

(18) Ermilov, V.; Lazutin, A.; Halperin, A. *Macromolecules* **2010**, *43*, 3511.

(19) Murat, M.; Grest, G. S. *Macromolecules* **1996**, *29*, 8282.

(20) Halperin, A.; Zhulina, E. B. *Langmuir* **2010**, *26*, 8933.

(21) $N_i = \int_{R_{core}}^{r_{co}} (\xi/a)^{5/3}\xi^{-1}\,\mathrm{d}r \approx f_{eq}{}^{-1/3}(r_{co}/a)^{5/3}[1 - (R_{core}/r_{co})^{5/3}] \approx \gamma^{3/5}N_B{}^{2/5}\varphi_A{}^{-5/4}(1 - \gamma^{-1/5}N_B{}^{1/5}\varphi_A{}^{3/4})$ and $N_i \ll N_A$ for $R_{micelle} \gg r_{co} \gtrsim R_{core}$.

(22) The elastic free energy of a chain of $\mathrm{d}n_{blob}$ ξ_A blobs at the interval r, $r + \mathrm{d}r$ is $\mathrm{d}F_{el}/kT = \xi_A{}^{-2}(\partial r/\partial n_{blob})^2\,\mathrm{d}n_{blob}$. Assuming the blobs are closed packed, $f_{eq}\xi_A{}^3\,\mathrm{d}n_{blob} \approx r^2\,\mathrm{d}r$, leads to $\mathrm{d}F_{el}/kT \approx f_{eq}\xi_A r^{-2}\,\mathrm{d}r$.

(23) Zhulina, E. B.; Adam, M.; LaRue, I.; Sheiko, S. S.; Rubinstein, M. *Macromolecules* **2005**, *38*, 5330.

(24) Halperin, A. *Macromolecules* **1989**, *22*, 3806.

(25) Abbas, S.; Lodge, T. P. *Phys. Rev. Lett.* **2007**, *99*, 137802.

(26) Abbas, S.; Lodge, T. P. *Macromolecules* **2008**, *41*, 8895.

(27) Camargo, M.; Likos, C. N. *Phys. Rev. Lett.* **2010**, *104*, 078301.